Biomaterials Science

PAPER

View Article Online
View Journal | View Issue

Check for updates

Cite this: *Biomater. Sci.*, 2019, **7**, 3249

Stacking up: a new approach for cell culture studies†

Diosangeles Soto Veliz, *[a] Hongbo Zhang [b,c] and Martti Toivakka[a]

Traditional cell culture relies mostly on flat plastic surfaces, such as Petri dishes and multiwell plates. These commercial surfaces provide limited flexibility for experimental design. In contrast, cell biology increasingly demands surface customisation, functionalisation, and cell monitoring in order to obtain data that is relevant *in vivo*. The development of research areas such as microfluidics and electrochemical detection methods greatly promoted the customised design of cell culture platforms. However, the challenges for mass production and material limitations prevent their widespread usage and commercialisation. This article presents a new cell culture platform based on stacks of a transparent flexible printable substrate. The arrangement introduces multi-layered stacks for possible manipulation and access to the cells. The platform is highly compatible with current technologies, such as colorimetric imaging and fluorescence microscopy. In addition, it can potentially integrate, *e.g.*, biomaterials, patterning, microfluidics, electrochemical detection and other techniques to influence, monitor, and assess cell behaviour in a multitude of different settings. More importantly, the platform is a low-cost alternative customisable through functional printing and coating technologies. The device shown in this manuscript represents a prototype for more sophisticated variations that will expand the relevance of *in vitro* studies in cell biology.

Received 28th December 2018,
Accepted 27th May 2019

DOI: 10.1039/c8bm01694a

rsc.li/biomaterials-science

Open Access Article. Published on 04 June 2019. Downloaded on 8/16/2025 7:18:16 PM.
This article is licensed under a Creative Commons Attribution-NonCommercial 3.0 Unported Licence.

1. Introduction

Over the past century, flat plastic surfaces, such as Petri dishes and multiwell plates, prevailed as cell culture platforms for cell growth, yet they still fail to mimic the *in vivo* cell behaviour. These platforms lack the physico-chemical properties of the extracellular environment that regulate cell fate.[1–3] Thus, they neglect the needs in experimental design for cell studies,[4] and prevent the translation of results to *in vivo* applications. In response, commercial alternatives have been developed for specific applications, such as cancer studies and co-cultures. The issue is that most of them share a common manufacturing technique: injection moulding. The process is accurate, fast and with some flexibility of design. However, it requires the creation of a mould for each design, thus limiting the freedom for customisation and functionalisation while increasing initial production costs. This means that research is constrained to the commercially predefined cell culture models despite the expanding needs in cell biology and advances in research areas such as microfluidics and sensing technologies.

Programmable and customised platforms for cell culture could potentially influence, manipulate, and monitor cell behaviour simultaneously. Such a device would overcome the fundamental limitations of conventional cell cultures. This ambition has led to the development of cell culture approaches capable to integrate functional biomaterials, printing, traditional microfluidics and electrochemical sensing.

Microfluidic research leads in applications such as high throughput screening,[5] single cell analysis,[6] organ-on-a-chip,[7] and radiation biology.[8] Polydimethylsiloxane (PDMS) is currently the material of choice for microfluidic devices, and a favourite to engineers due to its optical clarity, low cost, reproducibility, ease of use, and rapid prototyping. However, the major limitations of PDMS in cell culture are the permeability to water vapour and small hydrophobic molecules, unstable surface treatment or functionalisation, and uncrosslinked oligomers, all of which affects the resulting cell behaviour.[9,10] In addition, some of the devices are not compatible with the technologies commonly used in cell studies,[11] and the manufacturing methods are difficult to scale-up for mass production.[12,13] Therefore, despite the advances and advantages, cell culture platform design remains a challenge.[14] Other approaches include the use of hydrogels,[15] paper,[16] and other polymeric systems.[17]

[a]*Laboratory of Paper Coating and Converting, Åbo Akademi University, Porthaninkatu 3, 20500 Turku, Finland. E-mail: diosangeles.sotoveliz@abo.fi*
[b]*Department of Pharmaceutical Science Laboratory, Åbo Akademi University, Tykistökatu 4, 20520 Turku, Finland*
[c]*Turku Center for Biotechnology, University of Turku and Åbo Akademi University, Tykistökatu 4, 20520 Turku, Finland*

† Electronic supplementary information (ESI) available: Appendix A, video A. See DOI: 10.1039/c8bm01694a

Open Access Article. Published on 04 June 2019. Downloaded on 8/16/2025 7:18:16 PM.
This article is licensed under a Creative Commons Attribution-NonCommercial 3.0 Unported Licence.

Recently, wax printing has emerged as an alternative approach to develop cell culture platforms. The method is largely used in paper-based microfluidics due to its low cost, simplicity, and speed of production.[18–20] In 2011, Derda *et al.* used wax printing to design a high-throughput paper-based 3D cell culture platform based on Cells-in-Gel-in-Paper (CiGiP).[21] The principle was to use the hydrophobic wax as a barrier to create hydrophilic zones for cells to grow. Since then, wax printing is extensively used in paper-based 3D cell culture studies. The next step is to exploit the benefits of using wax printing methods for cell culture and expand its applications to cell patterning,[22] and to create microwells for cell studies.[23]

This article shows an easy to manufacture, scalable, customisable alternative to current cell culture platforms. The device takes advantage of commercialised techniques such as wax printing, and desktop cutting. Once assembled, the platform is compatible with current protocols and methods like microscopy and fluorescence detection. More importantly, it has the means to integrate numerous state-of-art technologies through large-scale fabrication techniques, such as functional printing and coating, thereby improving their accessibility into research.

2. Experimental

The proposed platform consists of multiple layers of flexible printable film stacked in a sandwich-like structure. Fig. 1a shows a graphical representation of the device and its layers, in addition to the side view of a single well after assembly of the stacked cell culture platform. The inner layers have specific patterns designed through cutting and serve as spacers in the device. The outer layers (base and cover) include printed hydrophobic boundaries to constrain the cell culture media (and cells) between these two surfaces. Herein, wax was used to create the hydrophobic boundaries, but it is exchangeable by any other hydrophobic material, *e.g.* PDMS.

Fig. 1b shows a summary of the design and fabrication of the cell growth platform. Initially, patterns are designed in Adobe Illustrator CC (Adobe Systems) and wax printed (ColorQube 8570, Xerox®). The layer designs used in this research are shown in Fig. A.1 of Appendix A.† However, the platform geometry can be modified to suit the intended investigation or analysis technique. It is possible, *e.g.*, to mimic 96-well plate geometry. In the case of larger designs, the device requires additional points of alignment since maintaining only the corners together will result in bending at the centre due to the film flexibility. After printing, the spacer layers are cut with a desktop cutter (Silhouette Curio™, Silhouette) according to the desired design (Silhouette Studio® Software, Silhouette). Before cell culture, the spacers are rinsed with 70% ethanol, and dried. Subsequently, all layers are sterilised with UV-C radiation in a laminar flow hood. Stitch pins are used (8 mm, platinum) to align and keep all layers together, but can be exchanged with other methods for alignment, such as a 3D printed case.

2.1. Characterisation of the substrate

The main component of the cell growth platform used herein is polyester film Melinex® OD (DuPont Teijin Films™) with a thickness of 125 μm. In principle, any transparent, printable, and biocompatible film, including flexible glass, could be used. Before use, the polyester film was washed with soap and tap water, followed by rinsing with deionised water, 70% ethanol, and drying. Wetting properties and surface chemistry of the washed polyester film as such, and after printing with black wax were characterised. PerkinElmer Lambda 900 spectrophotometer and PerkinElmer Spectrum One FTIR Spectrometer (ATR mode) were used to collect the UV/Vis and IR spectra, respectively. CAM 200 (KSV Instruments Ltd) was used to measure the contact angle at the following conditions: (a) before printing, (b) after printing, and (c) after contact with each one of four liquids: deionised water, phosphate buffer solution, serum-free cell culture media (SF), and complete cell culture media (COMP). Droplet size was 6 μL, and the wettability was quantified through the Young–Laplace equation.

2.2. Cell culture of human dermal fibroblasts

Human Dermal Fibroblasts (HDFs, ATCC® PCS-201-010™) were cultured in Dulbecco's Modified Eagle's Medium (DMEM, Sigma-Aldrich) with 10% Foetal Bovine Serum (FBS, Biowest), penicillin–streptomycin (10 000 units per 10 mg mL^{-1}, Sigma-Aldrich), and L-glutamine (200 mM, Biowest) as supplements. Cells were kept in an incubator (37 °C, 5% CO_2, and 95% relative humidity), and subcultured when 80–90% confluent.

2.3. Cell culture of HDFs in the stacked platform

Well areas in the plate were first pre-wet with DMEM. Then, cell seeding was increased per column (labelled 1 to 4 from left to right): 0 cells (1), 5000 cells (2), 10 000 cells (3), and 15 000 cells (4). The total liquid volume added to each well was 60 μL. Calcein AM (ThermoFisher Scientific) was used to stain the metabolically active cells after one and three days of cell culture. Briefly, a working solution in PBS of 5 μM Calcein AM was prepared from a stock solution of 1 mM Calcein AM. After five minutes of incubation in the working solution, the bottom layer of the plate was scanned (488 channel) with a ChemiDoc™ XRS+ System (Bio-Rad Laboratories). The data collected was analysed in Image Lab™ Software (Bio-Rad Laboratories). At each time point, cells were imaged using a ZEISS Axio Vert.A1 (ZEISS). Prior to imaging, a row of cells was treated with 50 μM cisplatin, a known inducer of apoptosis, and incubated for 10 hours.

2.4. Immunofluorescence staining

The well areas were pre-wet with DMEM prior to seeding the cells. The 13 mm inner wells contained 30 000 cells in a volume of 140 μL. The 7 mm outer wells had 30 μL of DMEM with no cells to prevent fast drying of the inner wells. As comparison, 30 000 cells in a volume of 500 μL were seeded in 13 mm coverslips placed in a 24-well plate. After one day of

 This journal is © The Royal Society of Chemistry 2019

Open Access Article. Published on 04 June 2019. Downloaded on 8/16/2025 7:18:16 PM.
This article is licensed under a Creative Commons Attribution-NonCommercial 3.0 Unported Licence.

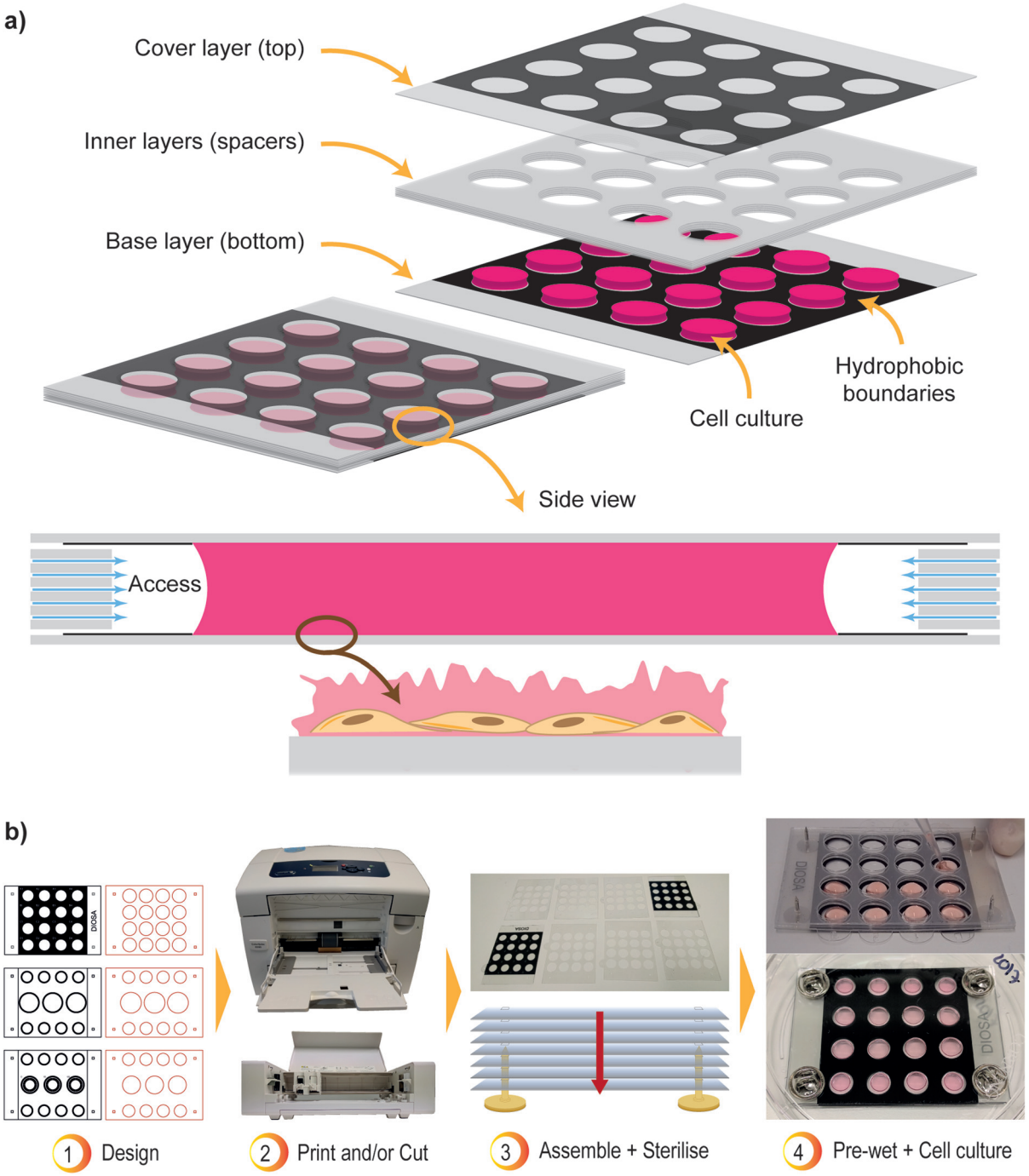

Fig. 1 Description of the cell growth platform. (a) Schematic representation of the stacked platform and its layers. It includes a side view representation to scale of a single well of the device. (b) General design and fabrication of the plastic-based cell growth platform.

incubation, cells were washed with PBS, fixed with 4% PFA in PBS for 15 minutes at room temperature, and washed repeatedly with PBS. Afterwards, cells were blocked, permeabilised and stained for one hour with 10% FBS, 0.3% Triton X-100, and 1 : 500 Alexa Fluor™ 555 Phalloidin (Invitrogen™, ThermoFisher Scientific) in PBS. Next, cells were incubated for five minutes with 300 nM DAPI (ThermoFisher Scientific) in PBS for nuclear staining, and later washed with PBS. Finally, the samples were mounted on microscope slides with Mowiol+DABCO (Sigma-Aldrich). Acquisition of the images was done with a 3i spinning disk microscope.

2.5. Assessment of hypoxia

Well areas of two plates were pre-wet with DMEM prior to seeding the cells. Cell seeding was of 15 000 cells in a volume of 100 µL per well. After one day of cell culture, one plate had a

Open Access Article. Published on 04 June 2019. Downloaded on 8/16/2025 7:18:16 PM.
This article is licensed under a Creative Commons Attribution-NonCommercial 3.0 Unported Licence.

change of media (untreated samples) and the other plate was treated with 1 mM fresh solution of $CoCl_2$ in DMEM to chemically induce hypoxia. Cells were incubated for 24 hours, washed with PBS, fixed with 4% PFA in PBS for 15 minutes at room temperature and washed repeatedly with PBS. Samples were blocked/permeabilised with 10% FBS, and 0.3% Triton X-100 in PBS for 30 minutes. Then incubated overnight at 4 °C with anti-HIF-1 alpha antibody [EPR16897] (dilution 1 : 100, Abcam) in PBS. The following day, after repeated washes in PBS, the samples are incubated for one hour at room temperature with 10% FBS, and goat anti-Rabbit IgG (H + L) secondary antibody Alexa Fluor Plus 555 (dilution 1 : 100, ThermoFisher Scientific) in PBS. Next, cells were stained with DAPI, washed with PBS, and mounted on microscope slides with Mowiol+DABCO. Acquisition of the images was done with a 3i spinning disk microscope. The post-processing was done with FijiImageJ,[24,25] using the median filter and Li method of threshold[26] to obtain the outline of the nuclei.

3. Results and discussion

This section starts with the characterisation of the stacked cell culture platform, followed by a discussion on the performance of the device during the cell culture, and comparison to current methods. Finally, some of the potential future modifications and applications of the platform are proposed.

3.1. Characterisation of the stacked cell culture platform

Microscopy is one of the main techniques utilised to monitor cell behaviour. Therefore, the use of a very thin and highly transparent material with optical clarity is an advantage in the fabrication of a cell culture platform. Fig. 2 shows the transmittance and ATR-FTIR spectra of the materials in the stacked cell culture platform (Melinex® OD and black wax). Most common excitation wavelengths in fluorescence microscopy are between 400–700 nm. Within that range, Melinex® OD has transmittance around 88%. This value is comparable to 90 and 91% given by the commercial cell culture plate (Greiner CELLSTAR®), and the glass coverslip, respectively (Fig. 2a). Below 400 nm, the transmittance for Melinex® OD decreases somewhat faster than for the other materials. If needed, materials with larger spectral window could be utilized. As expected, the printed black wax has very low transmittance below 650 nm. The purpose of using wax is to create hydrophobic boundaries to constrain the liquid and cells into wells rather than serve as a cell growth surface. Therefore, the low transmittance in the black wax printed areas does not represent a limitation for observing the cells.

The ATR-FTIR spectra confirms the composition of the Melinex® OD and the wax (Fig. 2b).[27] Peaks from Melinex® OD are representative of polyester films including *C–O* stretching (1097–1244 cm^{-1}), *C–H* bending (1340–1409 cm^{-1}), *C=C* aromatic stretching (1505–1578 cm^{-1}), *C=O* stretching (1715 cm^{-1}), and *C–H* stretching (2907–2969 cm^{-1}). Peaks from the black wax are similar to those of paraffin. The peaks

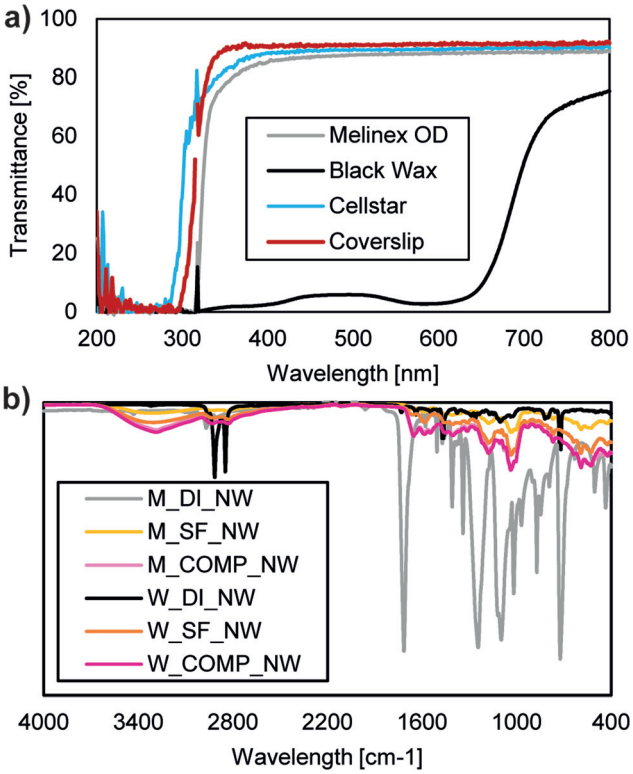

Fig. 2 Characterisation of the materials in the stacked platform. (a) Transmittance spectra of Melinex® OD, black wax-printed Melinex® OD, commercial cell culture plate (Cellstar), and glass coverslip between 200 and 800 nm. (b) ATR-FTIR spectra of Melinex® OD (M) and black wax-printed Melinex® OD (W) after contact with dionised water (DI), serum free DMEM (SF), and complete DMEM (COMP), and no washes (NW).

include the CH_2 in plane rocking band (719–730 cm^{-1}), *C–H* bending vibration (both asymmetric and symmetric) from CH_2 groups (1472 cm^{-1}), *C–H* bending vibrations from CH_3 groups (1378–1462 cm^{-1}), strong *C–H* stretching vibrations (both asymmetric and symmetric) from the CH_2 groups (2847–2866 cm^{-1}), and CH_3 stretching vibrations (2955 cm^{-1}). Other bands present in the wax spectra are possibly from the black pigment compound of the ink and weaker methylene bands at 1350–1150 cm^{-1}.

The ATR-FTIR spectra shows changes in the surface chemistry after contact with both cell culture media (Fig. 2b). Despite the differences between Melinex® OD and the black wax ink, both materials have similar spectra after exposure to the cell culture media. The change is not permanent, and it is possible to reverse it through multiple washes by deionised water (Appendix A, Fig. A.2†). Since the changes occur for DMEM with and without serum, the adsorption of molecules is not just the proteins in the serum but also other compounds present in the serum free DMEM. Serum free DMEM contains inorganic salts, amino acids, vitamins and other additives such as phenol red, glucose and penicillin–streptomycin. Therefore, it is difficult to single out specific adsorbed compounds from the complex mixture.

 This journal is © The Royal Society of Chemistry 2019

Open Access Article. Published on 04 June 2019. Downloaded on 8/16/2025 7:18:16 PM.
This article is licensed under a Creative Commons Attribution-NonCommercial 3.0 Unported Licence.

Table 1 Contact angle measurements for Melinex® OD and black wax printed surfaces before and after contact with deionised water (DI), phosphate buffer (PBS), serum free DMEM (SF), and complete DMEM (COMP)

Sample	DI	PBS	SF	COMP
Melinex® OD	88 ± 0.9	89 ± 0.3	88 ± 1	91 ± 2
Melinex® OD after liquid	89 ± 2	85 ± 2	80 ± 3	8 ± 2.8
Black wax	112 ± 1.3	110 ± 0.4	110 ± 2	105 ± 0.8
Black wax after liquid	110 ± 1	102 ± 0.8	12 ± 2	14 ± 2

Contact angle measurements help further understand the changes to the surface chemistry induced by the cell culture media. Table 1 shows the contact angles at 10 seconds after droplet placement for the Melinex® OD and black wax printed surfaces before and after contact with the liquids. In this case, the liquids considered were deionised water (DI), phosphate buffered solution (PBS), serum free DMEM (SF), and complete DMEM (COMP).

The contact angle of both surfaces decreases significantly after contact with the cell culture media. This change confirms the interaction seen in the ATR-FTIR spectra. In the implementation of the stacked platform, the cell culture media does not cover the black wax. Therefore, despite the possible interactions between the wax and the media, the black wax can still form the boundaries of the wells. In the case of the Melinex® OD, the initial contact angle is not hydrophilic enough to promote spontaneous wetting and spreading of the liquid on the surface. Functional coatings on the film surface before wax printing are possibilities to enhance the wetting. In this case, it was enough to pre-wet the wells with cell culture media before cell seeding.

3.2. Manufacture and implementation of the stacked cell culture platform

The prototype device was manually assembled using a wax printer for the hydrophobic boundaries, and a desktop cutter for the layers. The material costs include the wax solid ink and the flexible printable film. The ink cost is about 0.85 EUR m^{-2} of substrate considering 20% coverage, while the flexible film used was about 1.18 EUR m^{-2}. Therefore, the material cost per device is about 0.11–0.13 EUR assuming that 16–18 devices (5 cm × 7 cm) are made from 1 m^2 of film. However, the device in its current state requires further considerations, such as the steps of manufacture, method of alignment, the time of design and customisation, and manual assembly.

Manufacture of the stacked cell culture platform for laboratory scale was straightforward and successful. See Appendix A, Video A.† for a demonstration of the platform. The design of the layers changed according to the purpose of the platform as explained in the Experimental section. The size of the cell staining wells meant for fixation was equivalent to a coverslip 13 mm, No. 1 in order to use the latter one as a control, except for the hypoxia studies. Higher magnifications of the wax printed designs showed uneven coverage by the fused wax ink toner particles (Appendix A, Fig. A.3†). The toner particle size and spreading during fusing partially define the resolution limitations of the used printing method to approximately 100 μm.

In the device, the cell culture media is pinned to the base and cover layer by the hydrophobic boundaries, and further kept in place by surface tension, as shown in Fig. 1a. This defines the volume of the well which depends on the ratio between the radius of the well and the gap between the cover and base layers. If the gap is too large, the surface tension is insufficient to keep the liquid between the layers. If the gap is too small, then the amount of liquid might not be enough to counter or delay the drying promoted by the airflow between the layers. Additionally, the shape of the hydrophobic boundaries, or wells, will affect the successful containment of the liquid.

Alignment of all the layers depend on the cutting resolution of the used cutter. The positioning of the layers is important since any contact between the inner layers and the cell culture media results in a fast lateral spreading of the liquid. In this study, a 1 mm distance between the printed well edges and the holes from the inner layers was enough to restrain the liquid within the hydrophobic boundaries, prevent any contact with the spacers, and correct any misalignments from the cutting process. An alternative approach could utilise hydrophobic material as spacer layers.

Fig. 3 summarises the results obtained from implementing the platform for cell culture. Pre-wetting of the surface prior to the addition of cells resulted in an evenly distributed cell seeding. The distribution is visible in both the imaging and scanning of the HDFs stained with Calcein AM. Fig. 3a shows images after one and three days of cell culture. Cells have the characteristic spindle-shape of HDFs and proliferate towards confluency by day three. This is suggested by the increased coverage of cells in the wells. Therefore, the device is suitable for the cell culture of HDFs. The method sufficed to maintain a contamination-free environment. It was possible to observe minor scratches and defects on the plastic substrate (not shown), yet they were not detrimental for the imaging. Images of cisplatin-treated HDFs can be found in Fig. A.4 of Appendix A.†

Quantification of the scanned surface revealed an increasing mean intensity proportional to the increase in cell amount (Fig. 3b). The linear increase makes it possible to create a standard curve to measure cell proliferation in future drug-screening studies. In the current setup and used liquid volumes, cell culture is possible up to three days before significant drying in the outer wells (Appendix A, Fig. A.5†). This period is enough for a wide range of assays that study cell behaviour. Longer cell culture times require manual change of cell culture media or the future design of an (semi)automatic fluid handling method.

Immunofluorescence microscopy is a method widely used by researchers. Therefore, it is important to ensure that the proposed device is compatible with the technique. Imaging of cells grown on Melinex® OD showed lower resolution than imaging of cells on coverslips when using the traditional sample preparation (Fig. 3c). Traditional sample preparation for imaging includes mounting fixed/stained cells directly to

Open Access Article. Published on 04 June 2019. Downloaded on 8/16/2025 7:18:16 PM.
This article is licensed under a Creative Commons Attribution-NonCommercial 3.0 Unported Licence.

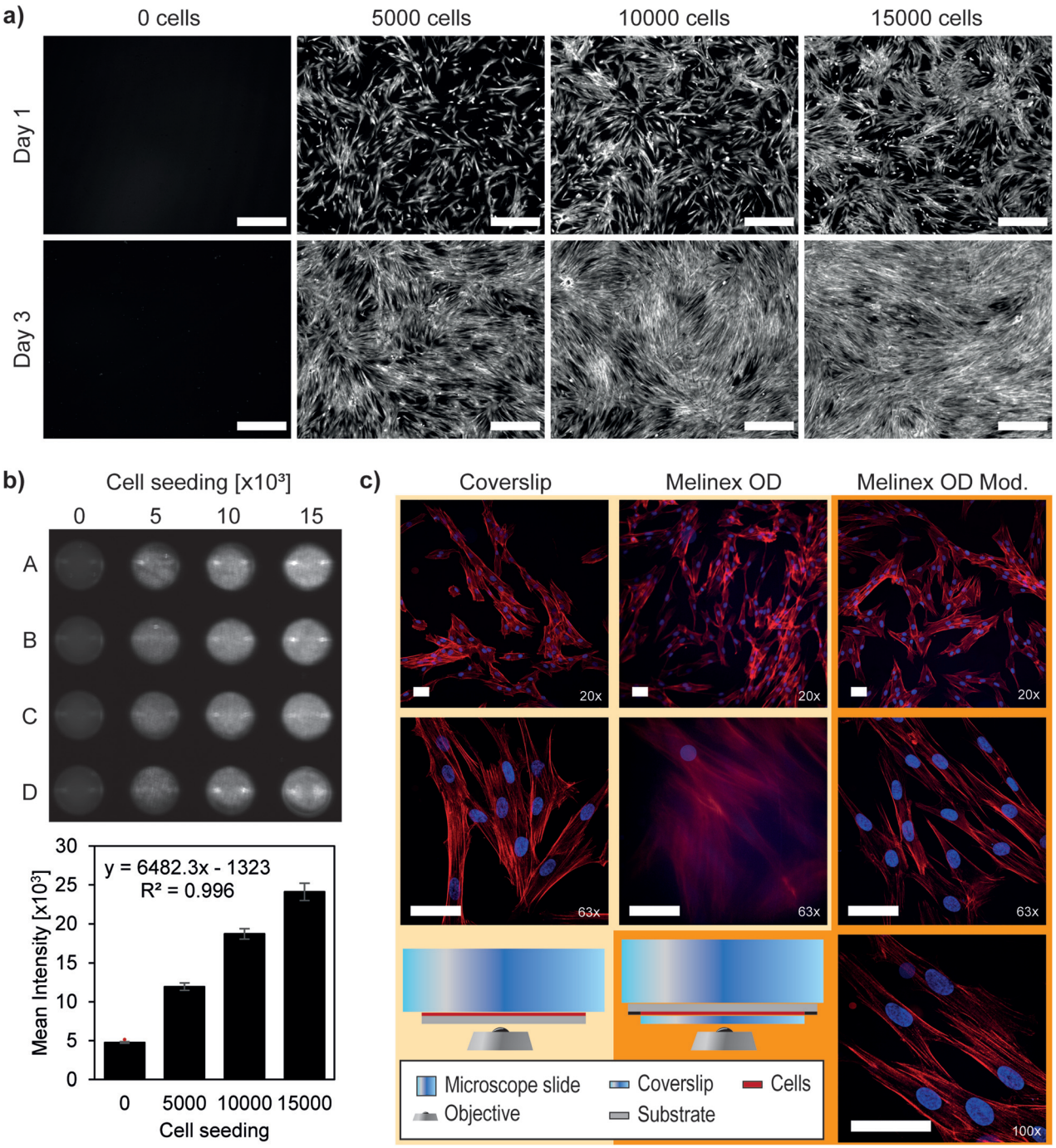

Fig. 3 Implementation of the cell culture platform. (a) Fluorescence imaging of HDFs stained with Calcein AM for a cell seeding of 0, 5000, 10 000, and 15 000 cells after one and three days of cell culture. Scale: 500 μm. (b) Fluorescence scanning and intensity quantification (linear fit) of HDFs stained with Calcein AM for a cell seeding of 0, 5000, 10 000, and 15 000 after one day of cell culture. (c) Spinning disk microscope images of HDFs stained for nucleus (DAPI, blue) and actin filaments (Alexa Fluor, red). Each image includes a scale of 50 μm in the bottom left corner, and the power of the objective used in the bottom right corner. This section also contains the schematic setups used for imaging the cells: the traditional method (coverslip, and Melinex® OD), and a modified version (Melinex® OD Mod.).

the microscope slide. The location of the cells is between the growth substrate and the microscope slide; therefore, in an inverted microscope, the imaging is done through the substrate. Microscope objectives and immersion oils are mostly designed to improve imaging through glass. Coverslip glass has a thickness between 130–160 μm, high spectral transmission, and a refractive index of approximately 1.5230. In contrast, Melinex® OD has a thickness of 125 μm, slightly lower spectral transmission, and a refractive index over 1.6, and haze of 0.4%, according to the manufacturer. The differ-

 This journal is © The Royal Society of Chemistry 2019

Open Access Article. Published on 04 June 2019. Downloaded on 8/16/2025 7:18:16 PM.
This article is licensed under a Creative Commons Attribution-NonCommercial 3.0 Unported Licence.

ences between the materials result in the loss of imaging resolution when imaging through the substrate.

It is possible to increase the compatibility of the stacked cell culture platform for high-resolution imaging by modifying the traditional sample preparation method. The substrate is mounted on the microscope slide with the fixed/stained cells facing outwards. Then, a coverslip is mounted on top of the cells. Consequently, the cells are located between the substrate and a coverslip, but the imaging occurs through the coverslip. The result are images with a resolution comparable to the ones obtained by growing cells on coverslips and with no interferences from the substrate even when using 100× objectives and immersion oil. Another future alternative is to replace the plastic film in the device with thin flexible glass substrate, which both maximizes the optical imaging resolution and maintains modification options through printing and solution processing techniques.

At last, it is important to consider the oxygen availability to the cells inside the device. At the moment, the layers are not sealed together and there is access for oxygen in between them, as shown in Fig. 1a. The separation between the layers is possibly due to the elevated edges created during the cutting step of manufacture. The effect is also noticeable by the increased and faster drying of the wells close to the edges (Appendix A, Fig. A.5†). The uneven drying raises a concern of hypoxic condition to the cells in the inner wells.

Fig. 4 shows the immunofluorescence staining of cells in a side well, and at the centre of the stacked cell culture platform. As a control, hypoxia was chemically induced in another device at the same locations. The images show that under hypoxic conditions HIF-1 alpha relocates to the nuclei, as reported in previous literature.[28] In comparison, cells cultured normally in the device show no accumulation of the protein in the nuclei. This indicates that the cells do not undergo hypoxia.

3.3. Future applications of the stacked cell culture platform

Compared to traditional, and PDMS cell culture platforms, the device proposed in this study provides a wider range of programmability to experimental design (Table 2). Geometrical modifications and printed wax barriers for channels can enable use of passive or active microfluidics in the device. Exchanging

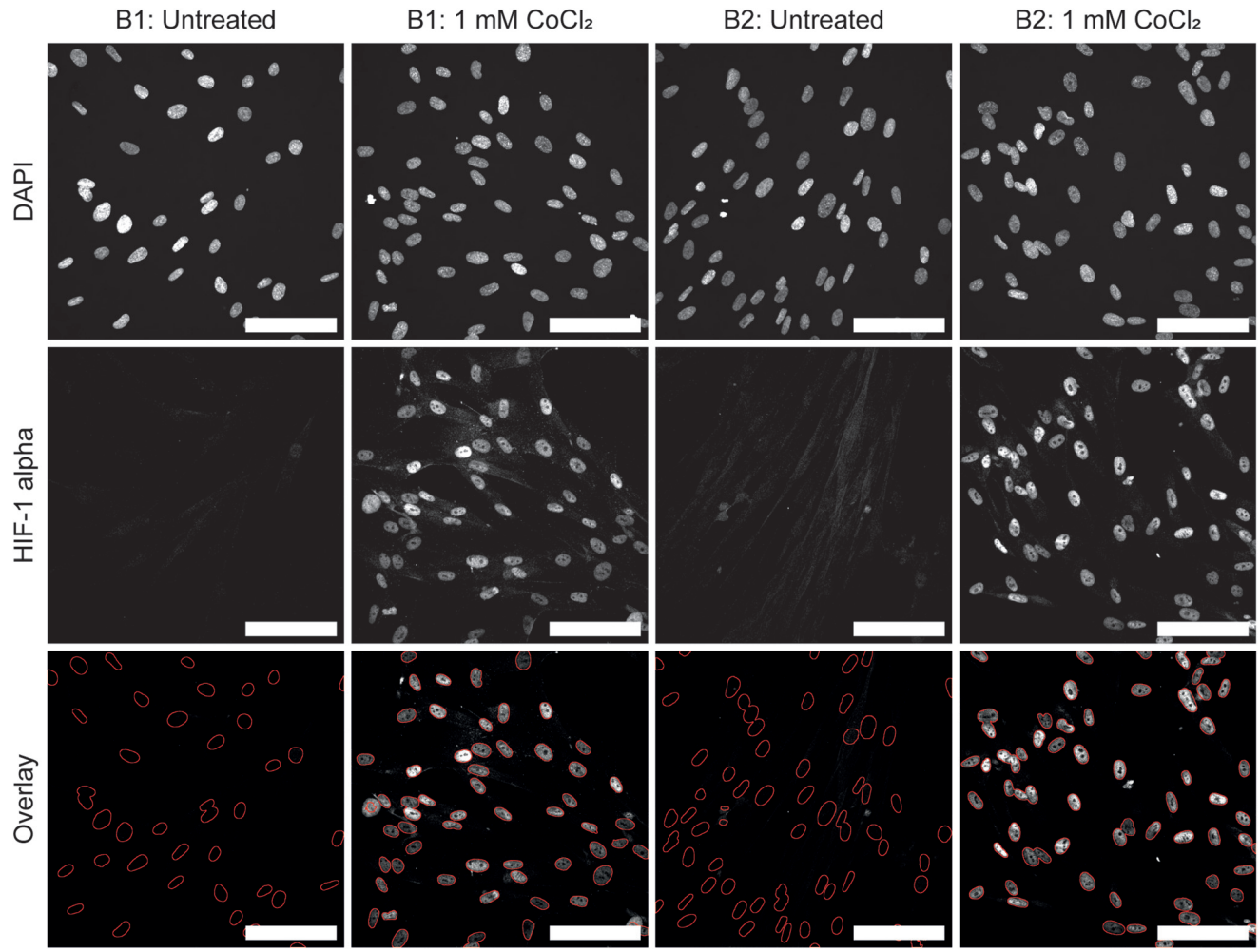

Fig. 4 Spinning disk images of untreated cells, and cells treated with 1 mM of $CoCl_2$. Cells were imaged from position B1 (side of the device), and B2 (centre of the device). The staining included DAPI for nuclei, and HIF-1 alpha as an indicator of hypoxia when relocalised to the nuclei. In addition, the figure includes an overlay of the nucleus outline on the HIF-1 alpha staining. Scale bar: 100 μm.

Open Access Article. Published on 04 June 2019. Downloaded on 8/16/2025 7:18:16 PM.
This article is licensed under a Creative Commons Attribution-NonCommercial 3.0 Unported Licence.

Table 2 Comparison between traditional cell culture, and the stacked cell culture

Parameter	Traditional cell culture	PDMS devices	Stacked cell culture
Cell number	Thousands to tens of millions	Single cells to tens of thousands	Single cells to tens of thousands
Gas transport	Irregular and governed by free convection (uncontrollable due to large liquid volumes)	Customisable through modifications to the design	Potentially customisable through modifications to spacer geometries and dynamic control due to low liquid volumes
Geometry	Predefined mould design	Predefined mould design	Size and shape can be altered for each design
Growth area	Limited to the bottom of the wells and the media suspension	Depends on the design	Both cover and base layer, in addition to the media suspension
Manufacture	Defined geometries mostly through injection moulding	Cross-linking of liquid PDMS into moulds and heated to replicate the mould geometry	Customisable through cutting/printing of flexible films
Material	Stiff polystyrene/glass	PDMS	Any flexible printable film
Scalability	Each design requires an investment for a different mould	Each design requires the making of a different mould	Compatible to a wide range of roll-to-roll process techniques, such as laser cutting and in-line printing. However, challenging due to assembly
Surface modifications	Possible through drop casting	Unstable modifications due to hydrophobic recovery	Possible through traditional and commercial techniques suitable for flexible films, such as coating and printing
Volume	High volume to area of cell growth ratio	Low volume to area of cell growth ratio	Low volume to area of cell growth ratio

the base layer for flexible glass would increase imaging resolution and use of porous materials in inner layers potentially introduces lateral communication between wells. The platform requires low volume of cell culture media and provides additional areas for cell growth. Cells can be attached to both the base and cover layer before the assembly of the stacked plate, and if necessary, suspension cells can be grown as well between the layers. This is potentially useful for the study of co-cultures of different cells lines and to mimic *in vivo* environments.

The printability of the platform is another benefit over traditional and PDMS cell culture, since it allows for the modification and functionalisation of the cell growth surface. Printed patterns inside the wells can separate the cells into smaller clusters or be used to study cellular processes like migration. Printed functional biomaterials or molecules can be assessed in the device or be used to regulate cell behaviour. Inclusion of electrochemical detection, such as thin, organic and large area electronics (TOLAE) technologies, is also possible through printing of solution processable materials. This can be particularly useful to monitor cells, and assess responses to different types of stimulations such as currents and lasers. In summary, the potential applications for the stacked platform include co-cultures, functional printing, patterning, electrochemical detection, and biofluidics.

Considering the future prospects, the proposed platform is an attractive alternative to current methods. Further studies and modifications are needed to exploit the potential of the device. However, the simplistic approach together with the ease of production and scalability make it a feasible new approach to cell culture studies.

4. Conclusions

This article introduces a new platform for cell culture studies. The device is easy to manufacture, customisable, and potentially scalable. It consists of stacks of a flexible printable film including two outer layers and multiple inner layers used as spacers. The outer layers include printed hydrophobic barriers to constrain the cell culture media in wells. The experiments showed that the platform, even in its basic form, is compatible with fluorescence measurements and microscopy. Further modifications to the platform would allow long-term studies, and the introduction of co-cultures, functional printing, fluid handling and electrochemical detection.

The proposed device represents an alternative to current platforms for cell culture. Its fabrication is potentially scalable to large volumes while still maintaining the freedom of design brought about by digital printing and converting technologies. From a research perspective, the device provides the means to include state-of-art technologies and expand their access to researchers in biological sciences.

Conflicts of interest

There are no conflicts to declare.

Acknowledgements

Thanks to the Doctoral Network of Material Sciences (Åbo Akademi University, Finland), Otto A. Malm Foundation, Alfred Kordelin Foundation, and the Finnish Foundation for Technology Promotion for the financial support. Prof. Zhang acknowledges the financial support from Academy of Finland (Grant No. 297580) and Sigrid Jusélius Foundation (decision no. 28001830K1). We also thank the FunMat Consortia for their support, and the Laboratory of Prof. John Eriksson where the biological studies took place. The imaging was conducted partially at the Cell Imaging Core from Turku Bioscience, Finland.

 This journal is © The Royal Society of Chemistry 2019

Open Access Article. Published on 04 June 2019. Downloaded on 8/16/2025 7:18:16 PM.
This article is licensed under a Creative Commons Attribution-NonCommercial 3.0 Unported Licence.

References

1 J. M. Muncie and V. M. Weaver, in *Chapter One – The Physical and Biochemical Properties of the Extracellular Matrix Regulate Cell Fate*, ed. E. Litscher and P. Wassarman, Academic Press, US, 1st edn, 2018, pp. 1–37.
2 D. J. Huels and J. P. Medema, *Cell Stem Cell*, 2018, **22**, 7–9.
3 G. Charras and E. Sahai, *Nat. Rev. Mol. Cell Biol.*, 2014, **15**, 813.
4 A. Abbott, *Nature*, 2003, **424**, 870.
5 G. Du, Q. Fang and J. M. J. den Toonder, *Anal. Chim. Acta*, 2016, **903**, 36–50.
6 A. Reece, B. Xia, Z. Jiang, B. Noren, R. McBride and J. Oakey, *Curr. Opin. Biotechnol.*, 2016, **40**, 90–96.
7 N. S. Bhise, J. ao Ribas, V. Manoharan, Y. S. Zhang, A. Polini, S. Massa, M. R. Dokmeci and A. Khademhosseini, *J. Controlled Release*, 2014, **190**, 82–93.
8 J. Lacombe, S. L. Phillips and F. Zenhausern, *Cancer Lett.*, 2016, **371**, 292–300.
9 E. Berthier, E. W. K. Young and D. Beebe, *Lab Chip*, 2012, **12**, 1224–1237.
10 K. J. Regehr, M. Domenech, J. T. Koepsel, K. C. Carver, S. Ellison-Zelski, W. L. Murphy, L. A. Schuler, E. T. Alarid and D. J. Beebe, *Lab Chip*, 2009, **9**, 2132–2139.
11 J. ryul Choi, H. Song, J. H. Sung, D. Kim and K. Kim, *Biosens. Bioelectron.*, 2016, **77**, 227–236.
12 H. F. Chan, S. Ma and K. W. Leong, *Regener. Biomater.*, 2016, **3**, 87–98.
13 L. R. Volpatti and A. K. Yetisen, *Trends Biotechnol.*, 2014, **32**, 347–350.
14 S. Halldorsson, E. Lucumi, R. Gómez-Sjöberg and R. M. T. Fleming, *Biosens. Bioelectron.*, 2015, **63**, 218–231.
15 S. R. Caliari and J. A. Burdick, *Nat. Methods*, 2016, **13**, 405.
16 K. Ng, B. Gao, K. W. Yong, Y. Li, M. Shi, X. Zhao, Z. Li, X. Zhang, B. Pingguan-Murphy, H. Yang and F. Xu, *Mater. Today*, 2017, **20**, 32–44.
17 J. Li, X. Fan, L. Yang, F. Wang, J. Zhang and Z. Wang, *Int. J. Polym. Mater. Polym. Biomater.*, 2018, **67**, 371–382.
18 E. Carrilho, A. W. Martinez and G. M. Whitesides, *Anal. Chem.*, 2009, **81**, 7091–7095.
19 W. Dungchai, O. Chailapakul and C. S. Henry, *Analyst*, 2011, **136**, 77–82.
20 T. Songjaroen, W. Dungchai, O. Chailapakul and W. Laiwattanapaisal, *Talanta*, 2011, **85**, 2587–2593.
21 R. Derda, S. K. Y. Tang, A. Laromaine, B. Mosadegh, E. Hong, M. Mwangi, A. Mammoto, D. E. Ingber and G. M. Whitesides, *PLoS One*, 2011, **6**, e18940.
22 C. C. W. Tse, S. S. Ng, J. Stringer, S. MacNeil, J. W. Haycock and P. J. Smith, *Int. J. Bioprint.*, 2015, **2**, 35–44.
23 A. Z. Qamar, K. Amar, P. Kohli, F. Chowdhury and M. H. Shamsi, *RSC Adv.*, 2016, **6**, 104919–104924.
24 C. T. Rueden, J. Schindelin, M. C. Hiner, B. E. DeZonia, A. E. Walter, E. T. Arena and K. W. Eliceiri, *BMC Bioinf.*, 2017, **18**, 529.
25 J. Schindelin, I. Arganda-Carreras, E. Frise, V. Kaynig, M. Longair, T. Pietzsch, S. Preibisch, C. Rueden, S. Saalfeld, B. Schmid, J.-Y. Tinevez, D. J. White, V. Hartenstein, K. Eliceiri, P. Tomancak and A. Cardona, *Nat. Methods*, 2012, **9**, 676–682.
26 C. Li and P. Tam, *Pattern Recognit. Lett.*, 1998, **19**, 771–776.
27 M. R. Derrick, D. C. Stulik and J. M. Landry, *Infrared spectroscopy in conservation science*, The Getty Conservation Institute, Los Angeles, 1999.
28 P. J. Kallio, K. Okamoto, S. O'Brien, P. Carrero, Y. Makino, H. Tanaka and L. Poellinger, *EMBO J.*, 1998, **17**, 6573–6586.